Chinese Chemical Letters 33 (2022) 4116–4120

Contents lists available at ScienceDirect

Chinese Chemical Letters

journal homepage: www.elsevier.com/locate/cclet

One-pot synthesis of concentration and excitation dual-dependency truly full-color photoluminescence carbon dots

Chen Wei[a,1], Shun Hu[a,1], Fuxin Liang[b], Zhining Song[b,*], Xue Liu[a,*]

[a] Institute of Clean Energy Chemistry, Key Laboratory for Green Synthesis and Preparative Chemistry of Advanced Materials, College of Chemistry, Liaoning University, Shenyang 110036, China
[b] Institute of Polymer Science and Engineering, Department of Chemical Engineering, Tsinghua University, Beijing 100084, China

ARTICLE INFO

Article history:
Received 25 September 2021
Revised 16 January 2022
Accepted 17 January 2022
Available online 23 January 2022

Keywords:
Carbon dots
Full-color
Fluorescent centers
Concentration and excitation
White-light LEDs

ABSTRACT

The paper describes a kind of truly full-color photoluminescence (PL) CDs. The CDs were prepared by using one-pot hydrothermally heating citric acid and formamide at 200 °C for 2 h. The CDs have three fluorescent centers at blue, green, and red light region. Their color was regulated through two means, including changing excitation wavelengths or CDs concentrations. The emission maxima changed from blue to red with the increase of excitation wavelengths or CDs concentrations. The full-color PL behavior of the CDs was inherited and conserved in the solid polymer matrix, giving multicolor CDs/polymer films and light emitting diodes (LEDs). White-light LED (WLED) with the CIE coordinate approaching to (0.31, 0.32) were also achieved.

Multicolor luminescent materials have received significant attention due to their broad application in sensing, bioimaging, full-color displays, light-emitting diodes, and optoelectronic devices [1–6]. In these multicolor luminescent materials, rare-earth based nanoparticles, semiconductor quantum dots and organic fluorescent dyes have been developed [7–10]. However, these luminescent materials often have many problems such as poor water solubility, complex preparation procedures, or high bio-toxicity [7–15]. Moreover, current methods for regulating the colors of these materials are also limited. Therefore, it remains challenges to develop novel multicolor luminescent materials with high utility and rich color regulation.

Carbon dots (CDs) as a novel type of multicolor luminescent materials have many remarkable advantages, such as superior optical properties, good solubility and biocompatibility, compared with traditional multicolor luminescent materials [16–20]. The preparation procedures of CDs are simple and easy, and their raw materials are abundant [21,22]. Hence, it is easier to prepare CDs with multicolor luminescence by choosing appropriate carbon source or controlling reaction conditions. A great variety of CDs with full-color emission (blue-red light region) have been successfully prepared by adjusting starting materials [23,24], reaction condition [25,26], or separation method (path-A) [27]. Lin's group synthesized three types of CDs inducing emissions in red, green and blue (RGB) three primary colors of luminescence through solvothermal treatment of three different phenylenediamine isomers as carbon sources [23]. Sun *et al.* prepared multiple-color-emission CDs by regulating the thermal-pyrolysis temperature of citric acid and urea [26]. Ding *et al.* reported that a kind of full-color light emitting CDs, which were hydrothermally synthesized in one pot and separated *via* silica column chromatography [27]. Besides, some CDs can also achieve multicolor luminescence by changing the excitation wavelength [28,29], solvents [30,31], or CDs concentration [32,33] (path-B). Pan *et al.* prepared excitation-dependent truly full-color CDs presenting unusually comparable emission intensity nearly across the entire range of visible spectrum [29]. Wang *et al.* synthesized excitation-independent multicolor emissive CDs, which showed different color emissions in different solvents or polymer matrixes [30]. Chen *et al.* reported concentration-dependent multicolor CDs with emissions changing from blue to orange light [33]. Both these two methods (path-A and path-B) contribute significantly to the development of full-color CDs. Nevertheless, each of these methods has its own advantages and drawbacks. The full-color CDs from path-A (CDs-A) are generally able to access various color emissions with high intensity and efficiency. However, various colors of CDs-A are actually achieved from a group of CDs, and such kind of full-color CDs is suitable for full-color displays. On the other hand, the full-color CDs from path-B (CDs-B) can directly achieve various color emissions from a sin-

* Corresponding authors.
E-mail addresses: songzhining@mail.tsinghua.edu.cn (Z. Song), liuxue@lnu.edu.cn (X. Liu).
[1] These authors contributed equally to this work.

https://doi.org/10.1016/j.cclet.2022.01.053
1001-8417/

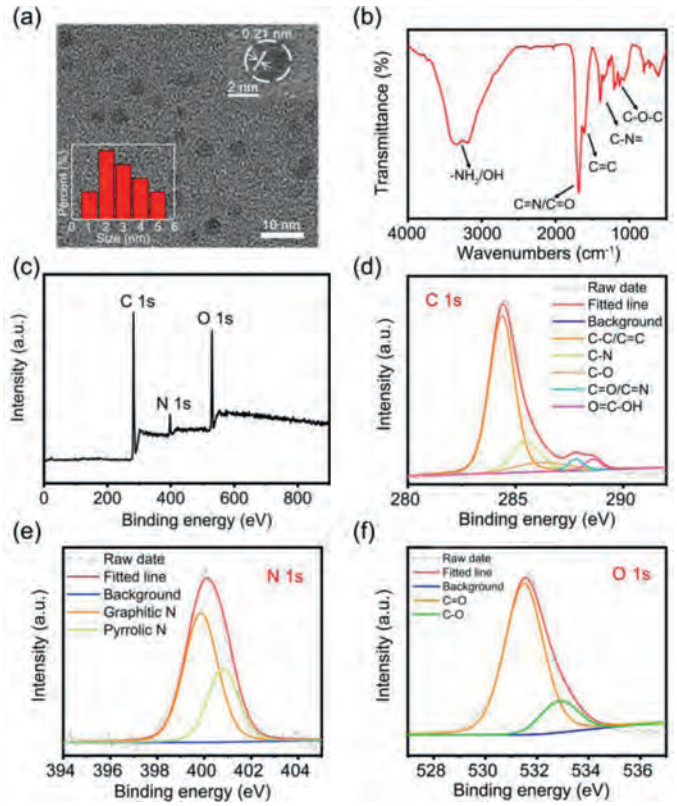

Fig. 1. (a) TEM image the CDs; inset: HRTEM image and the particle size histograms of the CDs. (b) FT-IR spectra of the CDs. (c) XPS full-survey; (d) high-resolution C 1s; (e) high-resolution N 1s; (f) high-resolution O 1s XPS spectra of the CDs.

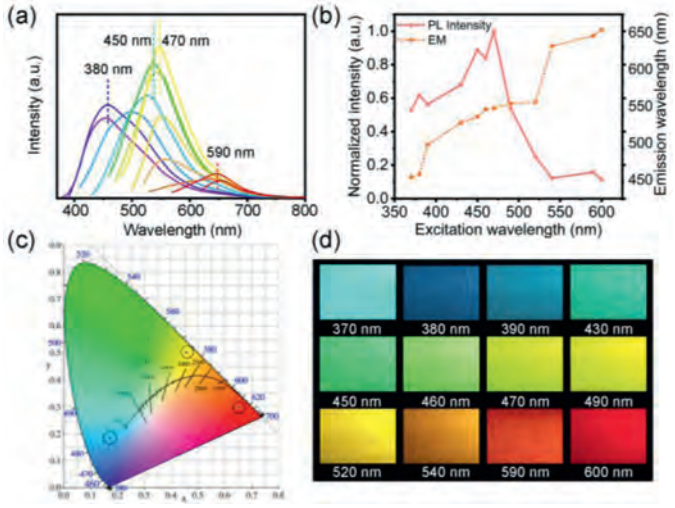

Fig. 2. (a) PL spectra of the CDs dispersed in ethanol solvent under different excitation wavelengths. (b) The maximum emissions under different excitation wavelengths and their corresponding normalized fluorescence intensity. (c) CIE chromaticity coordinate of blue, green, yellow, and red excited at the indicated wavelengths. (d) PL emission photographs of the CDs recorded under the excitation wavelengths from 370 nm to 600 nm.

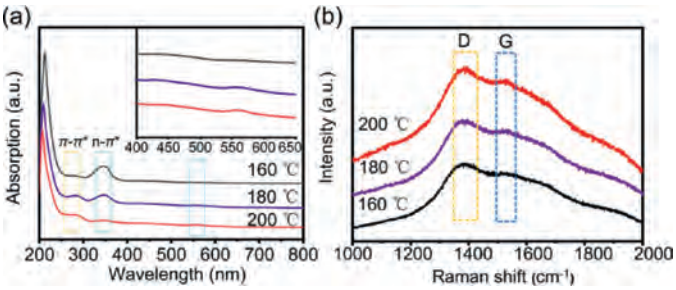

Fig. 3. (a) UV–vis absorption spectra of the CDs prepared at 160, 180 and 200 °C, respectively; (b) Raman spectra of the CDs prepared at 160, 180 and 200 °C, respectively.

gle CD. Such kind of full-color CDs is available for sensing through monitoring obvious stimuli-responsive color transition. Nevertheless, various colors of CDs-B are generally achieved from a fluorescent center, which results in low fluorescent intensity and efficiency of certain color emissions. Truly full-color CDs-B with multiple fluorescent centers at three primary colors were rarely reported. Truly full-color CDs can guarantee intensity and efficiency of various color emissions and have practical value.

Herein, we report a kind of concentration and excitation dual-dependency truly full-color fluorescent CDs *via* a one-pot solvothermal synthesis by using citric acid and formamide (Scheme S1 in Supporting information). The CDs present full-color emission from blue to green, yellow, and red with the increase of excitation wavelength and its concentration. The full-color CDs are confirmed to contain multiple fluorescence emission centers in the 2D fluorescent excitation-emission matrix. They can be applied in preparing full-color polymer films and LEDs.

The morphology and composition characterizations of the CDs including TEM, FT-IR and XPS were performed. The TEM image illustrates that the CDs are well-dispersed in ethanol (Fig. 1a), with average particle sizes of approximately 2.9 nm. The high-resolution TEM (HRTEM) image shows that the sample has similar well-resolved lattice fringes with a spacing of 0.21 nm, indicating the successful synthesis of well-crystallized CDs [34,35]. The FT-IR spectrum exhibits the characteristic absorption bands (Fig. 1b), including the stretching vibrations of C=N/C=O, C=C and C–N at 1680, 1605, and 1390 cm^{-1}, and the asymmetric and symmetric stretching vibrations of C–O–C at 1130 and 1075 cm^{-1}. The broad absorption bands from 3200 cm^{-1} to 3350 cm^{-1} indicate the presence of amino ($-NH_2$) and hydroxyl (–OH) functional groups on the surface of the CDs. Furthermore, the chemical compositions of the CDs were investigated by XPS analysis (Figs. 1c-f), which further support the FT-IR analysis. For instance, the CDs mainly contain C, O, and N elements (*i.e.*, C/O/N = 1.0/0.75/0.28, molar ratios). The typical high-resolution XPS C 1s spectrum can be deconvoluted into five binding energies (*i.e.*, C–C/C=C, 284.4 eV; C–N, 285.5 eV; C–O, 286.5 eV; C=N/C=O, 287.8 eV; –COOH, 288.6 eV) (Fig. 1d and Table S1 in Supporting information) [29,36]. In the high-resolution XPS N 1s, two fitting peaks at 399.8 and 400.8 eV are corresponding to the graphitic-like/amino N and pyrrolic-like N, respectively (Fig. 1e) [37]. The two fitting peaks of O 1s XPS at 531.5 and 532.8 eV are attributed to C=O and C−O bonds (Fig. 1f). These characterizations show the CDs compose of nano-scale graphite-like skeleton/core, and they are covered with N and O containing heterocyclic chemical structures and abundant amino and hydroxyl functional groups.

The excitation-dependent optical properties of the CDs were thoroughly investigated by fluorescence (FL), UV–vis absorbance and Raman analysis. As shown in Fig. 2a, there is no regular pattern in the variation of the fluorescence spectra of the CDs dispersed in ethanol solvent as altering the excitation wavelengths from 370 nm to 600 nm unlike most of the other CDs. The fluorescence emissions nearly cover the entire visible spectrum. The normalized maximum fluorescence intensities and their locations are provided in Fig. 2b and Fig. S1a (Supporting information) for allow-

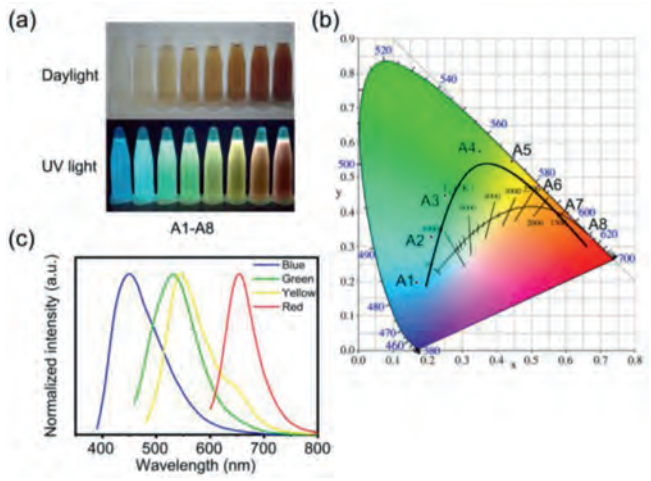

Fig. 4. (a) Photograph of the CDs ethanol solutions with various concentrations in daylight (upper) and 365 nm UV-light excitation (bottom). (b) CIE chromaticity coordinate of A1-A8 samples excited at the indicated wavelengths. The concentrations of A1-A8 samples are 0.0064, 0.0128, 0.0192, 0.032, 0.0448, 0.064, 0.128, and 0.192 mg/mL, respectively. (c) Normalized PL emission spectra of the A1 (Blue), A4 (Green), A6 (Yellow), and A8 (Red) samples under their optimum excitation wavelength.

ing easy observation. The emission wavelengths suffer a red-shift from 450 nm to 650 nm. Multiple platforms appear in the curve of the emission wavelength to excitation wavelength, demonstrating the CDs experience several fluorescence emitters. Under the combined effect of these emitters, all of these fluorescence spectra are asymmetric with a wide full width at half maximum (FWHM). From the curve of the fluorescence intensity to excitation wavelength, four peaks appear at 458, 536, 548, and 646 nm under the excitation wavelength of 380, 450, 470 and 590 nm, respectively. These four fluorescence spectra were converted to CIE coordinates to determine the exact spatial coordinates of the chromophores, and CIE color coordinates of blue (0.19, 0.21), green (0.34, 0.53), yellow (0.40, 0.55) and red (0.66, 0.31) emitters were achieved (Fig. 2c). These colors are readily observed by naked eye as well from the photographed cuvettes (Fig. 2d and Fig. S1b in Supporting information). The QYs of carbon dots under 380, 450, 470 and 590 nm are determined to be 11.1%, 21.3%, 15.9% and 9.4%, respectively.

The difference (ΔW) between the excitation wavelength and their maximum emission wavelength can reflect the degree of the excitation lights (Table S2 in Supporting information). The results show obvious variation in the corresponding differences among the various excitation lights, and again confirm the existence of multiple emitters. Moreover, it is obvious that the ΔW tend to converge when the emission wavelengths approach the optimum excitation wavelength of the corresponding emitters. This multicolor fluorescence phenomenon could be formed by the sp^2 carbon-induced variation in energy gaps between the π and π^* states [38,39]. The size of the sp^2 carbon domains can determine the quantum confinement effect of the CDs and drive their emission toward the light region with long emissions [3]. To elucidate the relationship between the sp^2 structure of the CDs and their luminescent behavior, several CDs were prepared with the same starting materials of equal amounts under different hydrothermal temperatures (Fig. S2 in Supporting information). The fluorescence emitters at three primary colors (red, green, and blue light) were compared at various preparation temperatures. The CDs at 160 and 180 °C show two main fluorescence emitters in the blue light and green light region; the CDs at 220 °C show three fluorescence emitters in the three primary color region similar to the above-mentioned CDs at

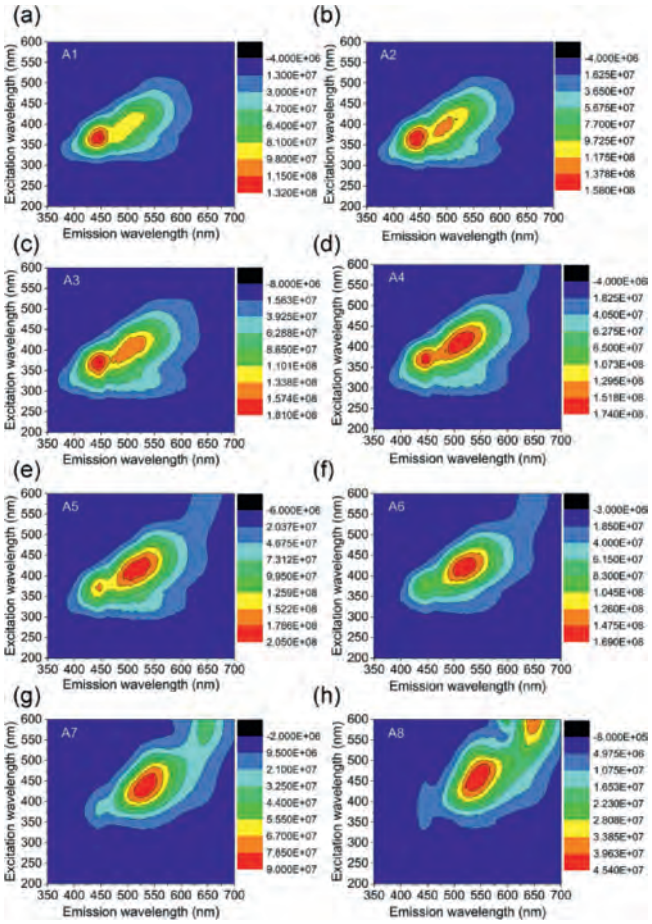

Fig. 5. 2D fluorescent matrix scan of the A1-A8 samples.

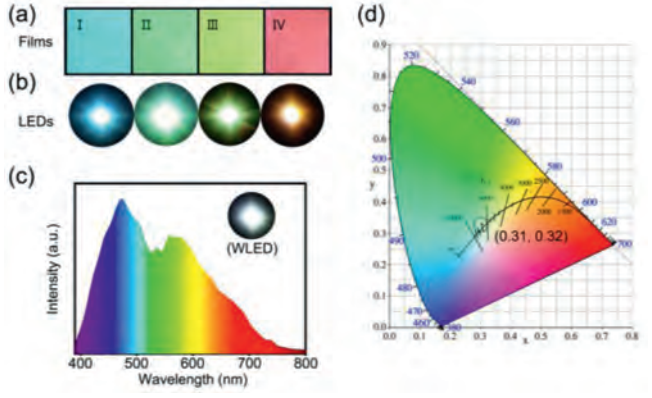

Fig. 6. (a) CDs/PVA films with multicolor emissions under the excitation of 365 nm UV-light; (b) blue-light, green-light, yellow light, and red-light LED prototypes. (c) WLED prototype and its solid-state emission spectrum. (d) CIE chromaticity coordinate of the WLED.

200 °C; the CDs at 240 °C show only one fluorescence emitter in the blue light region. Over-carbonization has occurred in the CDs at 240 °C, and makes them show monochromatic luminescence. The fluorescence emitter in the blue region appears in all of the CDs, and is hardly affected by their preparation temperatures. The fluorescence emitter in the green light region is underpowered by the high temperature. Conversely, the fluorescence emitter in the red light region is enhanced with the increasing preparation temperatures. The characteristic absorption in the UV–vis spectra can reflect the structural features of the CDs, including sp^2 structure

(Fig. 3a and Fig. S3 in Supporting information). In the UV region of 210–350 nm, a single peak is observed at 345 nm with a shoulder peak at 282 nm, corresponding to the n-π^* transition of the C=O bond and the π-π^* transition of the C=N bonds, respectively. With the increased preparation temperatures, the n-π^* peak is reduced while the π-π^* peak is elevated. The elevated π-π^* transition suggests an increased energy gap between the π and π^* states and an increased conjugated sp^2 domain [40]. Besides, the elevated visible absorption at 560 nm in the UV–vis spectra can also confirm the size increase of the conjugated sp^2 domain in the particles [23]. Fig. 3b shows the Raman spectra of three CDs at 160, 180 and 200 °C. The peaks at 1387 and 1525 cm^{-1} in the Raman spectra correspond to the disordered (D band) and graphite (G band) carbon in carbon materials [26,39]. The ratio of I_D/I_G is 1.12, 1.09 and 1.06 at 160, 180 and 200 °C, respectively. The decreased I_D/I_G also implies the increased number of embedded graphitic carbon atoms in the CDs with their increased preparation temperatures, that is, the increased conjugated sp^2 domain in the CDs.

The CDs present not only excitation-dependent luminescence, but also concentration-dependent luminescence. In order to investigate the concentration-dependent PL behavior of the CDs, we prepared a series of CDs ethanol solutions with the concentration of 0.0064, 0.0128, 0.0192, 0.032, 0.0448, 0.064, 0.128 and 0.192 mg/mL, respectively (A1-A8 samples). With the increased concentration of the CDs, the colors of CDs solutions gradually deepen in daylight (Fig. 4a, upper). Interestingly, under the excitation of 365 nm UV-light, the CDs solutions display full-color PL emission, which can be directly observed by naked eye as well (Fig. 4a, bottom). The increase in the CDs concentration leads to a red shift in their emission. Furthermore, the normalized PL emission spectra of the A1-A8 samples were recorded under the excitation wavelength of 400 nm (Fig. S4 in Supporting information), and the PL emission centers of the CDs exhibit gradual bathochromic shift with the increase of the CDs concentration. The fluorescence spectra were converted to CIE coordinates to determine the exact spatial coordinates of these CDs. Commission Internationale de L'Eclairage 1931 (CIE) coordinate of A1-A8 samples shows that the CDs excited at 400 nm can achieve full-color emission from blue to red (Fig. 4b). The corresponding CIE coordinates are (0.16, 0.19), (0.21, 0.32), (0.25, 0.44), (0.35, 0.57), (0.44, 0.54), (0.52, 0.47), (0.61, 0.38), and (0.67, 0.32), respectively. Four CDs samples (A1, A4, A6, and A8), their CIE color coordinates of blue, green, yellow, and red, were chosen to further investigate their PL properties in details. Under the optimum excitation wavelengths (λ_{oe}), their maximum fluorescence emissions (λ_{me}) are just located in the blue light (λ_{oe} = 380 nm, λ_{me} = 446 nm), green light (λ_{oe} = 450 nm, λ_{me} = 529 nm), yellow light (λ_{oe} = 470 nm, λ_{me} = 547 nm), and red light (λ_{oe} = 590 nm, λ_{me} = 653 nm) region, respectively (Fig. 4c). Their PL spectra under different excitation wavelengths and corresponding excitation-emission spectra under the λ_{oe} are shown in Figs. S5 and S6 (Supporting information). The CDs at lower concentrations (A1, A4 and A6) show three main fluorescence emitters in the blue light, green light, and red light region, and A8 sample show two main fluorescence emitters in the green light and red light region. With the raise of the concentration, the fluorescence emitters in the blue light region are gradually underpowered; those in the green light region increase first and then decrease; those in the red light region remain up-regulated. The UV–vis absorption spectra (Fig. S7 in Supporting information) of the CDs can illustrate the full-color fluorescence emissive phenomenon. The CDs with the emissions in the long-wavelength region have an obvious absorption peak in long wavelength, which may be attributable to the formation of large sp^2 conjugation [23,35]. With the increasing CDs concentration, the UV–vis absorption of the CDs in the long-wavelength region increases significantly.

To further investigate the mechanism of the concentration-dependent PL behavior of the CDs, specified 2D fluorescent matrix scans were performed on the A1-A8 CDs. The fluorescence center in the blue light region lies within the excitation wavelength range from 360 nm to 390 nm (Fig. 5a). A new fluorescent center appears in the green light region in A2 CDs (Fig. 5b). Clearly, the fluorescence center in the blue light and green light region are located at 447 and 515 nm, with the excitation wavelength of 375 and 415 nm, respectively. With the increase of CDs concentration (A1-A3), the emission intensity of the green fluorescent center gradually increases. The emission intensity is raised with the red shift of the emission wavelength (A4-A6), implying an effective energy transfer from blue light to green light region *via* a broad band absorption, which can be inferred from the UV–vis absorption spectra of the CDs in Fig. S7 (Supporting information). A further increase in CDs concentration causes the disappearance of the fluorescent emissive center in blue light region (A7). Next, the fluorescence emission center gradually shifts towards the red light region. A large irregular emission area in the red light region is observed in A8, showing a new fluorescent emissive center at 650 nm. The fluorescence center in the red light region can be assigned to the intrinsic energy level of the N-related defect states between surface bands [1].

It has been reported that the full-color PL behavior of the CDs can be extended to solid-state films for solid-state lighting. In this case, full-color emissive CDs/polyvinyl alcohol (PVA) composite films were successfully fabricated (Fig. 6a). PVA matrix favors the CDs with different concentrations to maintain their full-color PL behavior when the films are shaped [40]. Notably, the obtained CDs/PVA films inherit the concentration and excitation dual-dependency full-color PL behavior. With increased CDs concentrations, CDs/PVA films emit a strong light from blue to red under UV light of 365 nm. The normalized solid-state PL emission spectra of the CDs/PVA films show obvious red-shift from blue light region to red light region with the increased excitation wavelength (Fig. S8a in Supporting information). The corresponding CIE coordinates of the CDs/PVA composite films at different excitation wavelengths are (0.26, 0.35), (0.32, 0.50), (0.41, 0.52), and (0.54, 0.45), respectively (Fig. S8b in Supporting information). CDs-based LEDs with various color emissions were prepared by using the corresponding CDs/PVA films and InGaN LED chips centered at 365 nm. These LEDs emit bright blue light, green light, yellow light, and red light (Fig. 6b and Fig. S9 in Supporting information). Furthermore, by combining blue light and yellow light CDs/PVA films, WLED with the CIE coordinate approaching to (0.31, 0.32) were achieved (Figs. 6c and d), realizing the LEDs with full-wavelength emissions. In a word, the full-color CDs have proved promising and very useful in manufacturing forward-looking multicolor films and LEDs.

In summary, both concentration and excitation double-dependence fluorescent CDs with truly full-color emission have been synthesized through a simple one-pot hydrothermal method. The CDs with tunable fluorescence colors can achieve full-color PL emission (including three primary color emissions) by adjusting the excitation wavelength and concentration. The excitation and concentration double-dependence PL behavior of the CDs can be attributed to the multiple emission centers formed from the different-sized conjugated sp^2 domains of the CDs. It can be confirmed that there are three fluorescent centers in the CDs corresponding to blue, green, and red light region in the 2D fluorescent excitation-emission matrix. Based on the unique multicolor PL properties, the CDs/PVA films were prepared and show similar excitation and concentration double-dependence solid-state PL behavior. Meanwhile, LEDs and WLED based on the CDs/PVA films were also fabricated for multicolor lighting. These applications confirm the versatile functions and bright prospect of the CDs in multicolor prototypes.

Declaration of competing interest

The authors declare that they have no known competing financial interests or personal relationships that could have appeared to influence the work reported in this paper.

Acknowledgments

This work was supported by National Natural Science Foundation of China (No. 51873085) and Liaoning Revitalization Talents Program (No. XLYC2007056).

Supplementary materials

Supplementary material associated with this article can be found, in the online version, at doi:10.1016/j.cclet.2022.01.053.

References

[1] M.L. Aulsebrook, B. Graham, M.R. Grace, K.L. Tuck, Coord. Chem. Rev. 375 (2018) 191–220.
[2] S.Y. Lu, L.Z. Sui, J.J. Liu, et al., Adv. Mater. 29 (2017) 1603443.
[3] X. Yang, L.Z. Sui, B.Y. Wang, et al., Sci. China Chem. 64 (2021) 1547–1553.
[4] P. He, Y.X. Shi, T. Meng, et al., Nanoscale 12 (2020) 4826–4832.
[5] B.Y. Wang, J.K. Yu, L.Z. Sui, et al., Adv. Sci. 8 (2020) 2001453.
[6] T.L. Feng, S.Y. Tao, D. Yue, et al., Small 16 (2020) 2001295.
[7] J. Kido, Y. Okamoto, Chem. Rev. 102 (2002) 2357–2368.
[8] Z.Y. Lv, Y. Wang, J.R. Chen, et al., Chem. Rev. 120 (2020) 3941–4006.
[9] L.H. Qu, X.G. Peng, J. Am. Chem. Soc. 124 (2002) 2049–2055.
[10] Y.H. Yan, X.Y. He, J.Y. Miao, et al., J. Mater. Chem. B 7 (2019) 6585–6591.
[11] F.L. Yuan, Y.K. Wang, G. Sharma, et al., Nature Photon 14 (2019) 171–176.
[12] Y.X. Zheng, K. Arkin, J.W. Hao, et al., Adv. Opt. Mater. 11 (2021) 2100688.
[13] Y.N. Zhao, C.L. Ou, J.K. Yu, et al., ACS Appl. Mater. Interfaces 13 (2021) 30098–30105.
[14] P. Senellart, G. Solomon, A. White, Nature Nanotech. 12 (2017) 1026–1039.
[15] B. Zheng, Y.F. Kang, T. Zhang, et al., Anal. Chem. 92 (2020) 5258–5266.
[16] T.V. de Medeiros, J. Manioudakis, F. Noun, et al., J. Mater. Chem. C 7 (2019) 7175–7195.
[17] P.G. Luo, S. Sahu, S.T. Yang, et al., J. Mater. Chem. B 1 (2013) 2116–2127.
[18] X.K. Xu, Y.D. Li, G.Q. Hu, et al., J. Mater. Chem. C 8 (2020) 16282–16294.
[19] W.D. Li, Y. Liu, B.Y. Wang, et al., Chin. Chem. Lett. 30 (2019) 2323–2327.
[20] K.M. Chan, W. Xu, H. Kwon, A.M. Kietrys, E.T. Kool, J. Am. Chem. Soc. 139 (2017) 13147–13155.
[21] H. Nie, M.J. Li, Q.S. Li, et al., Chem. Mater. 26 (2014) 3104–3112.
[22] K. Lee, E. Park, H.A. Lee, et al., Nanoscale 9 (2017) 16596–16601.
[23] K. Jiang, S. Sun, L. Zhang, et al., Angew. Chem. Int. Ed. 127 (2015) 5450–5453.
[24] Z. Tian, X.T. Zhang, D. Li, et al., Adv. Opt. Mater. 5 (2017) 1700416.
[25] H. Ding, J.S. Wei, P. Zhang, et al., Small 14 (2018) 1800612.
[26] X. Miao, D. Qu, D.X. Yang, et al., Adv. Mater. 30 (2018) 1704740.
[27] H. Ding, S.B. Yu, J.S. Wei, H.M. Xiong, ACS Nano 10 (2016) 484–491.
[28] Y.P. Sun, B. Zhou, Y. Lin, et al., J. Am. Chem. Soc. 128 (2006) 7756–7757.
[29] L.L. Pan, S. Sun, A.D. Zhang, et al., Adv. Mater. 27 (2015) 7782–7787.
[30] M. Moniruzzaman, J.S. Kim, Sens. Actuators B: Chem. 295 (2019) 12–21.
[31] D.Y. Chao, W. Lyu, Liu Y.B, et al., J. Mater. Chem. C 6 (2018) 7527–7532.
[32] X. Meng, Q. Chang, C.R. Xue, J.L. Yang, S.L. Hu, Chem. Commun. 53 (2017) 3074–3077.
[33] Y.Q. Chen, H.Z. Lian, Y. Wei, et al., Nanoscale 10 (2018) 6734–6743.
[34] D. Gao, Y.S. Zhang, A.M. Liu, et al., Chem. Eng. J. 388 (2020) 124119.
[35] L. Wang, W.T. Li, L.Q. Yin, et al., Sci. Adv. 6 (2020) eabb6772.
[36] S. Sun, L. Zhang, K. Jiang, A.G. Wu, H.W. Lin, Chem. Mater. 28 (2016) 8659–8668.
[37] P. Lesani, G. Singh, C. Viray, et al., ACS Appl. Mater. Interfaces 12 (2020) 18395–18406.
[38] Y.N. Hong, J.W.Y. Lam, B.Z. Tang, Chem. Soc. Rev. 40 (2011) 5361–5388.
[39] P. Zhao, X.P. Li, G. Baryshnikov, et al., Chem. Sci. 9 (2018) 1323–1329.
[40] K. Hola, M. Sudolska, S. Kalytchuk, et al., ACS Nano 11 (2017) 12402–12410.